ENERGY STORAGE IN CORONAL FIELDS DUE TO CHANGING DOMAIN FLUXES

Lucas Tarr & Dana Longcope

Department of Physics, Montana State University

Abstract

The Minimum Current Corona (MCC) model provides a way to estimate stored coronal energy using the number of field lines connecting regions of positive and negative photospheric flux. This information is quantified by the net flux connecting pairs of opposing regions in a connectivity matrix. Changes in the coronal magnetic field, due processes such as magnetic reconnection, manifest themselves as changes in the connectivity matrix. However, the connectivity matrix will also change when sources emerge or submerge through the photosphere, as often happens in active regions. We have developed an algorithm to estimate the changes in flux due to emergence and submergence of magnetic flux sources. These estimated changes must be removed in order to quantify storage and release of magnetic energy in the corona. To perform this calculation over extended periods of time, we must additionally have a consistently labeled connectivity matrix over the entire observational timespan. We have therefore developed an automated tracking algorithm to generate a consistent connectivity matrix as the photospheric source regions evolve over time.

Magnetic Charge Topology

We can describe photospheric/coronal fields, and their evolution, topologically. The topology of a region derives directly from photospheric sources. Approximating unipolar regions as point sources allows one realistically quantify magnetic flux connecting those regions and, most important for the present work, changes in those interconnections. This is known as Magnetic Charge Topology (MCT). Figure 1 shows an example of mapping an MDI magnetogram to a set of point sources which match an extrapolated photospheric field to the dipole term.

Rigorous definitions of relevant topological terms—nulls, spines, fans, separators, &c.—can be found in Longcope&Klapper[1]. The connection of a field's topological entities define its skeleton, and example of which is shown at two different times for AR 10488 and AR10493 in Figure 2.

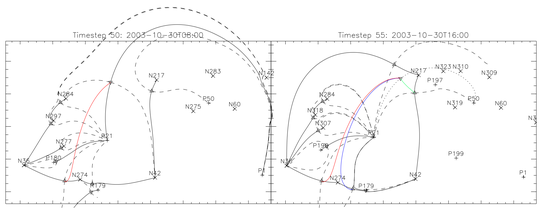

Figure 2: Topological skeleton of a subsection of Figure 1. Solid lines are spines, dashed lines fans, and the dotted line in the right hand panel is a coronal spine, which includes a coronal null connected to three separators. Separators are shown in color.

Minimum Current Corona[2][3]

While MCT provides a model for determining the initial topology of a source region, we need an additional model to track and quantify changes in the topology and the causes of those changes. The MCC model provides a framework for this second step[4]. It is a self–consistent, analytic model of quasi–static 3–D field evolution, which relies on two assumptions:

1. Photospheric field is composed of discrete, unipolar regions surrounded by a contiguous region of zero vertical flux
2. The corona evolves quasi–statically through a series of flux–constrained equilibria (FCE), fields with the lowest magnetic energy that still match the photospheric boundary and contain the prescribed distribution of domain fluxes

The coronal field resulting from assumption 2 is current–free except along separators of the field. The separators store energy in both the current sheet and magnetic tension. The FCE fields have the same domains as a potential field, but with different domain fluxes. The FCE field is defined to minimize the magnetic energy, constraining each domain flux to remain constant under variation of the vector potential $\mathbf{A}$.

Contact

Lucas Tarr
PhD Student

email: ltarr@physics.montana.edu
address: Montana State University
Department of Physics
Bozeman, Mt 59715
phone: 971.533.0469

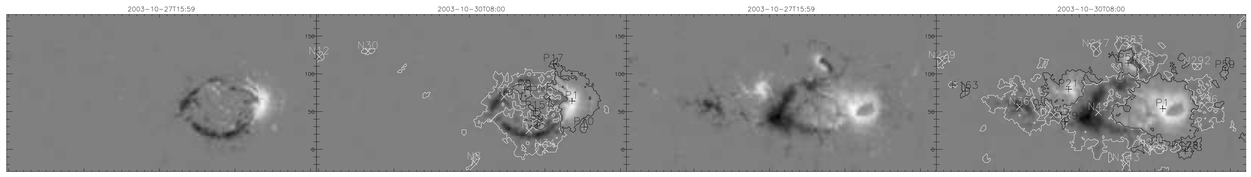

Figure 1: Section of the solar surface encompassing AR10488 and 10493, before and after partitioning, at two different times. Crosses and pluses show the centroid location of each region, where each region's associated pole is placed. Distance measured in Mm from disc center.

Data preparation

We track a region of the photosphere, in accordance with the sun's rotation, over a number of days, constituting N timesteps. At each timestep, we break the resulting magnetogram into unipolar regions via the downhill tesselation algorithm described in Barnes et al. 2005[5]; this defines a mask at each timestep identifying every pixel in the magnetogram with a unique region. Each unipolar region is then described by a topological pole, located at the flux–weighted centroid of its corresponding region, and inheriting that region's unprojected flux. This process is depicted in Figure 1.

Consistency in time

Photospheric sources constantly grow and shrink, break up, combine, and change shape over time, as illustrated in Figure 1. Consistently identifying regions over time is correspondingly difficult, so we have 3 phenomenologically–developed algorithms that counteract the 3 most common causes of misidentification:

rmv_flick removes regions that exist for a single timestep. The transient region is merged with longer–lasting regions with which it overlaps

rmv_vanish relabels regions that exist for many timesteps and then abruptly change names

rmv_shift adjusts the boundary between two regions in an attempt to maintain the flux in each region

The first two algorithms, rmv_flick and rmv_vanish, have very similar behavior, as shown in Figure 3. They basically amount to automatic relabeling that mimics a simple, by–hand method.

Figure 3: Typical behavior of both the rmv_flick and rmv_vanish algorithms.

For rmv_shift we use a modified version of Algorithm 1. We identify pairs of neighboring like–polarity regions, where one has increased flux, and the other decreased. This implies a shifting boundary between the two masks, as opposed to some underlying change in the photospheric field. rmv_shift then adjusts the boundary to minimize the flux–change in each region, as illustrated in figure Figure 4.

Figure 4: Behavior of the rmv_shift algorithm, where the boundary between $P1$ and $P2$ has been manipulated in order maintain a more constant flux in each region.

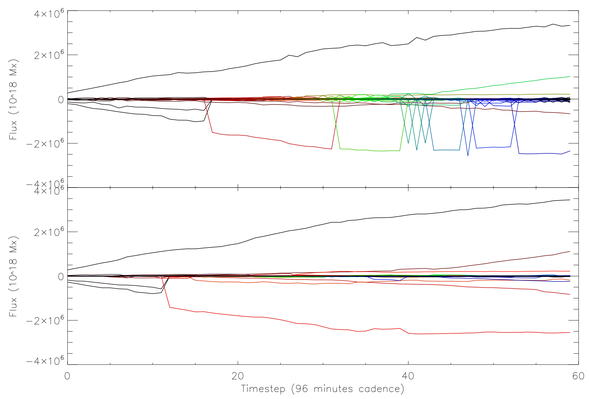

Figure 5: Each plot shows the flux in each unipolar region a section of the photosphere encompassing NOAA active regions 10488 and 10493 for MDI magnetograms, at a 96 minute cadence, starting on 2003-10-26. Th upper plot is before filtering with the rmv_⋆ algorithms. The lower plot shows the effect of repeated passes with each of the algorithms. The timesteps shown are, from top to bottom, 10, 30, and 50. Before filtering, the 60 timesteps were populated with ≈ 1200 distinct unipolar regions, and afterwards with ≈ 550.

Accounting for photospheric changes

As demonstrated in both Figure 1 and Figure 5, the distribution, number, and size of photospheric sources change substantially over the course of days. We have an heuristic algorithm based on two assumptions: (1) photospheric sources emerge and submerge in pairs; and (2) sources with little flux change should be less connected than those with big change. Algorithm 1 provides a precise method for quantifying the amount of flux–change each pole undergoes due to sub/emergence with other poles.

Representing time with superscripts and poles with subscripts, for a set of poles $\{P\}$ with fluxes $\{\psi\}$, we do the following:

Algorithm 1: Quantifying Sub/emerging Flux Change

begin
  $\Delta\psi_j^i = \psi_j^{i+1} - \psi_j^i$: The flux–change for each pole between consecuative timesteps;
  repeat
    $P_c \leftarrow$ pole with smallest (but non–zero) changing flux, $d\psi_c$;
    Link P_c to its nearest neighbor of opposite polarity but same sense flux change, P_n;
    Cancel $d\psi_c$ from $\Delta\psi_c$ and $\Delta\psi_n$;
    $\Delta\mathbb{M}_{s_{c,n}} \leftarrow d\psi_c$;
  until *no more connections can be made.* ;
end

An example run of this algorithm is depicted in Figure 6. The Resulting flux change matrix for sources, $\Delta\mathbb{M}_s$, represents a map of submerging and emerging flux between pairs of poles.

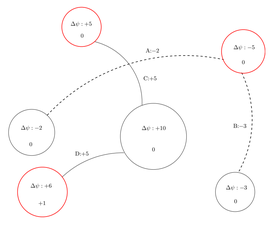

Figure 6: Example progression of the flux–change removal algorithm.

In the figure at left, red and black circles represent positive and negative flux regions, respectively. Inside each circle, the top number is the pre–algorithm change in flux relative to a previous timestep; the bottom number is the flux change after sub/emerging pairs have been identified. Lines between circles represent elements of the flux–change matrix $\Delta\mathbb{M}_s$, and are ordered (A, B, C…) by participation in the algorithm. Numbers on each line indicate the strength of the connection. This example has a net amount $(+1)$ of emerging flux.

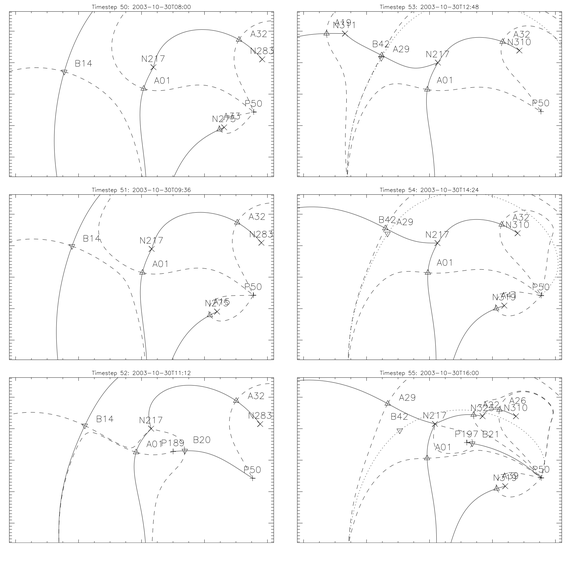

Figure 7: A pitchfork bifurcation, where a single photospheric null, B14 in the left panels, splits into a photospheric null of opposite type, A29, and a coronal null, B42, and a mirror null (not shown) in the right panels. and mirror null (not shown) of the original type. The coronal spine connects region P50 to P21.

Energetics

The domain fluxes can be calculated, eg., for a potential field, as described by Barnes et al. 2005[5]. The resulting matrix $\mathbb{M}_P^i$ represents the flux connecting each pair of poles at time i. The potential field's domain fluxes can change through two processes: a change in the photospheric sources, $\Delta\mathbb{M}_s^i$, or a change in the domain fluxes due to reconnection, $\Delta\mathbb{M}_{rx}$. Therefore, $\Delta\mathbb{M}_P^i \equiv \mathbb{M}_P^{i+1} - \mathbb{M}_P^i = \Delta\mathbb{M}_s + \Delta\mathbb{M}_{rx}$. The change in photospheric sources is just the sub/emerging connectivity we calculated above, so

$$\Delta\mathbb{M}_{rx}^i = \Delta\mathbb{M}_P - \Delta\mathbb{M}_s \tag{1}$$

The non–zero elements of the $\Delta\mathbb{M}_{rx}^i$ matrix are then the self–fluxes of current sheets formed at domain boundaries, or separators. For a separator of length L and current I the self–flux is

$$\Psi = \frac{IL}{4\pi}\ln\left(\frac{eI^\star}{|I|}\right) \tag{2}$$

from which the excess energy of the MCC field relative to the potential field is

$$\Delta W_{MCC} = \frac{1}{4\pi}\int_{\Psi_{potl}}^{\Psi} I d\Psi = \frac{LI^2}{32\pi^2}\ln\left(\frac{\sqrt{e}I^\star}{|I|}\right) \tag{3}$$

Both of the above equations, and the current $I^\star$, are derived and precisely defined in Longcope & Magara 2004[3].

Separator energy during a null bifurcation

The left panel of Figure 2 shows the skeleton for a subsection of the magnetogram shown on the right in Figure 1, encompassing poles N36 to P1, and up to N217, which the right panel shows the same region a few hours later; in color are the separators, which, after the pitchfork bifurcation shown in Figure 7, rise into the corona. Using the methond described above, we have calculated the energy stored at the separator for both the separators shown at timestep 50 and for the red+green union of separators at time 55, in Figure 2.

To our knowledge, this is the first time a null bifurcation has been derived from observation, and the first time the energy stored in a separator passing through a coronal null has been calculated.

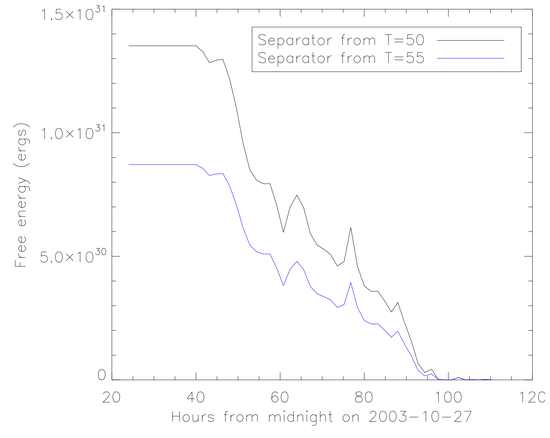

Figure 8: A null bifurcation, where a single photospheric null (B14, B24, &B28 in the left panels) splits into a photospheric null of opposite type (A29, A11, and A23 in the right panels), and a coronal null (shown; B42 and B43 in the right panels) and mirror null (not shown) of the original type.

References

[1] D.W. Longcope and I. Klapper. A general theory of connectivity and current sheets in coronal magnetic fields anchored to discrete sources. *ApJ*, **579**:468, 2002.

[2] D.W. Longcope. Topology and curreng ribbons: A model for reconnection and flaring in a complex, evoloving corona. *SolPhys*, **169**:91, 1996.

[3] D.W. Longcope and T. Magara. A comparison of the minimum current corona to a magnetohydrodynamic simulation of quasi–static coronal evolution. *ApJ*, **608**:1106, 2004.

[4] D. W. Longcope. Separator current sheets: Generic features in minimum-energy magnetic fields subject to flux constraints. *Physics of Plasmas*, **8**:5277–5290, December 2001.

[5] G. Barnes, D.W. Longcope, and K.D. Leka. Implementing a magnetic charge topology model for solar active regions. *ApJ*, **629**:561, 2005.

This work was supported by NASA Living With a Star.